Inverse Design of Spectrally Selective Thickness Sensitive Pigmented Coatings for Solar Thermal Applications

Refet A. Yalçın, Hakan Ertürk[1]
Boğaziçi University, Department of Mechanical Engineering
Bebek 34342 Istanbul, Turkey

ABSTRACT Inverse design of thickness sensitive spectrally selective pigmented coatings that are used in absorbers of solar thermal collectors is considered. The objective is to maximize collection efficiency by achieving high absorptance at solar wavelengths and low emittance at the infrared wavelengths to minimize heat loss. Radiative properties of these coatings depend on coating thickness, pigment size, concentration, and the optical properties of binder and pigment materials, and a unified radiative transfer model of the pigmented coatings is developed in order to understand the effect of these parameters on the properties. The unified model relies on Lorenz-Mie theory for independent scattering regime in conjunction with extended Hartel theory to incorporate the multiple scattering effects, T-matrix method for dependent scattering and effective medium theory for very small particles. A simplified version of the unified model ignoring dependent scattering is also developed for improving computational efficiency. Through the solution of the radiative transfer equation by the four flux method, spectral properties is predicted. The developed model is used in conjunction with inverse design for estimating design variables yielding the desired spectral emittance of the ideal coating. The nonlinear inverse design problem is solved by optimization by using Simulated Annealing method that is capable of finding global minimum regardless of initial guess.

Keywords: radiative transfer, pigmented coating, spectral tuning, solar absorber, Lorenz-Mie, T-matrix, four flux method, effective medium theory, inverse design, simulated annealing.

Nomenclature

$A_1,..,A_5$	Constants for four flux method
a_n, b_n	Lorenz-Mie coefficients
$C_0,..,C_2$	Constants for four flux method
C_f	Concentration factor of the concentrating solar collector
$C_{ext,\lambda}$	Spectral extinction cross section [m^2]
$C_{sca,\lambda}$	Spectral scattering cross section [m^2]
d_λ	Spectral dielectric function (relative permittivity)
$E_{b,\lambda}$	Spectral blackbody emissive power [W/m^2-μm]
$G_{s,\lambda}$	Spectral solar irradiance [W/m^2-μm]

[1] Corresponding Author
Tel: +90 212 359 7356
Fax: +90 212 287 2456
email: hakan.erturk@boun.edu.tr

$I_{c,\lambda}$	Collimated spectral intensity in +z direction [W/m^2-μm-sr]
$I_{d,\lambda}$	Diffuse spectral intensity in +z direction [W/m^2-μm-sr]
$J_{c,\lambda}$	Collimated spectral intensity in -z direction [W/m^2-μm-sr]
$J_{d,\lambda}$	Diffuse spectral intensity in -z direction [W/m^2-μm-sr]
$F(\boldsymbol{\chi})$	Objective function to be minimized
f_v	Pigment volume fraction
k	Extinction index of material
m	Relative complex refractive index of material
n	Refractive index of material
$p(\mu)$	Scattering phase function
r_p	Pigment radius [nm]
R_λ	Spectral reflectance
q''	Absorber net radiant flux [W/m^2]
t	Thickness of the coating [μm]
T_a	Absorber temperature [K]
x	Size parameter
V	Volume [m^3]

Greek Letters

α_λ	Spectral absorptance
β_λ	Spectral extinction coefficient [1/m]
$\boldsymbol{\chi}$	Unknown vector
ε	*Dielectric constant*
ϵ_λ	*Spectral emittance*
μ	$cos(\theta)$
σ_c	Forward scattering ratio for the collimated intensity
σ_d	Forward scattering ratio for the diffuse intensity
$\sigma_{s,\lambda}$	Spectral scattering coefficient [1/m]
θ	Polar angle
ρ_c	Boundary reflectivity for the collimated intensity from outside to coating
ρ_c'	Boundary reflectivity for the collimated intensity from substrate to coating
ρ_d	Boundary reflectivity for the diffuse intensity from coating to outside
ρ_d'	Boundary reflectivity for the diffuse intensity from coating to substrate
ξ	Average pathlength parameter

Subcripts and Suprescipts

c	collimated
cp	candidate point
d	diffuse
e	effective
ideal	Ideal coating property
λ	Spectral quantity
p	Pigment material
r	Resin material
s	Substrate material

1. Introduction

There has been growing concern on global climate change, availability of existing sources and environmental safety for the current energy infrastructure that predominantly rely on fossil fuel and nuclear technologies. These concerns have increased interest on utilization of renewable energy sources, and solar energy systems are considered as one of the leading alternatives. However, the most important roadblock for wide adoption of solar energy is considered as its relatively high cost per power. Reducing manufacturing costs and improving the performance of the systems are required to reduce the cost per power for solar technologies.

Solar thermal systems rely on transferring solar energy to a working fluid that is either used directly or in a thermodynamic cycle such as Rankine cycle for producing useful work. A brief review of solar thermal systems and their applications is presented in [1]. Concentrating systems such as parabolic-trough collectors are used to produce high temperature working fluids that is required for power cycles. The concentrator and absorber design must be optimized to maximize the amount of energy transferred to the working fluid and the performance of concentrating solar-thermal systems accordingly. However, majority of the installed solar thermal systems are for domestic water heating [2].

Special coatings are used for receivers to maximize absorption of incident solar energy. Depending on receiver temperature, energy loss by emission must also be minimized to maximize the net radiative transfer to the receiver and the working fluid. Therefore, spectrally selective coatings must have high absorptance at shorter solar wavelengths and low emittance at longer IR wavelengths. A detailed review of spectrally selective coatings for medium to high temperature concentrating solar systems is presented in [3].

Pigmented coatings comprise of a binder or a resin material and micro to nanometer sized particles known as pigments, and they are widely used as solar coatings due to their low cost [4]. The pigmented coating's radiative properties depend on pigment and resin materials' optical properties, pigment size and concentration, and the thickness of the coating. Therefore, optimizing a solar coating for maximizing the performance of the solar system necessitates the estimation of these parameters.

Radiative properties of solar coatings produced through different manufacturing processes were characterized experimentally in earlier studies such as [5], and thickness, volume fraction and radius are altered in various experimental and theoretical studies such as [6-8]. A summary of the earlier works on pigmented coatings with comparisons of effective medium theory (EMT) based predictions and experimental results are presented in [9]. While use of EMT is practical, it does not yield accurate predictions unless small pigments or infrared (IR) radiation is considered [10]. A more accurate prediction of the radiative behavior of pigmented coatings can be achieved using Lorenz-Mie theory (LMT) and Kubelka-Munk theory (KMT) considering independent single scattering. Kubelka-Munk theory is based on two-flux model and describes radiative behavior of thin translucent films subject to diffuse irradiation. Extended KMT considers collimated irradiation rather than diffuse [11] and therefore, it is more appropriate to use it for modeling solar coatings. The multiple scattering effects can be incorporated by extended Hartel theory (EHT) [12]. Using four-flux method (FFM) improves accuracy further considering both collimated and diffuse components of radiation [13], in conjunction with LMT and EHT [14]. When pigments are densely spaced with respect to the wavelength, the effects of dependent scattering must be

considered in IR wavelengths [15]. T-matrix method can be used in conjunction four flux method is used to estimate the spectral behavior of the coating [16].

The models proposed in [11-14] are applied to predict the spectral behavior of solar coatings [17], and their validation for polymer based TiO_2 or SiO_2 pigmented coatings for radiative cooling applications are presented in [18,19]. Effects of particle size and volume fraction is also presented through a parametric study [20]. More recently, LMT and radiation element method by ray emission model (REM^2) has been employed for optimizing TiO_2 based coatings for thermal and aesthetic effects, where radiative cooling is desired while minimizing the glare for buildings [21]. A comparison of CuO and TiO_2 pigmented coatings for radiative cooling are presented in [22], and a black-color coating with high reflectance in the NIR region is established by altering CuO particles' size in [23]. The optimal pigment size and concentration is identified through Nelder-Mead Simplex method and Quasi-Newton Opmization for various solar thermal applications to closely match ideal coating behavior relying on inverse design, where the system is modeled using LMT with EHT and FFM, considering a fixed coating thickness [24].

However, coating thickness also effects spectral coating's behavior and should also be optimized [25]. Thickness sensitive, spectrally selective solar coatings are investigated using LMT and FFM, estimating the solar absorptance and total emittance and a range where the optimal values of coating thickness, pigment radius and concentration for commonly used pigments are suggested based on a parametric study [26]. Optimizing pigmented coatings to obtain high transmission in visible wavelengths and low transmission in UV wavelengths by altering thickness, volume fraction and radius are considered in [27], where numerical calculations are compared with experimental measurements.

Considering the literature, this study first presents a unified model for predicting the spectral reflectance of the pigmented coatings considering EMT, independent, and dependent scattering regimes combining models developed in the earlier studies [11-14]. The unified model is then used for design of the spectrally selective coatings for solar thermal applications. Two different collector types; flat plate and parabolic trough collectors are considered to find optimum pigmented coating types at different conditions such as absorber temperature and solar irradiation. An ideal coating behavior, in terms of spectral emittance, is defined to maximize the net radiant energy transferred to the working fluid in solar thermal systems. The design problem is considered as predicting the pigment size, volume fraction and coating thickness that best approximates the ideal coating's net heat flux, and it is formulated as an inverse problem, where the cause of a known or desired effect is sought. This design is usually referred as inverse design was applied for radiative transfer problems earlier. Solution of non-linear inverse design problems is possible by optimization methods [28,29], and a global search algorithm, simulated annealing method (SAM), is used in this study as the introduction of thickness to the unknowns results in a topology with multiple local extrema.

2. Radiative Transfer Properties of Pigmented Coatings

The scattering behavior of particles can be classified according to their particle volume fraction and size parameter, $x=2\pi n r_p/\lambda$, using the regime map introduced by Tien and Brewster [30]. Three regions of interest for pigmented coatings are those where EMT, independent multiple scattering and dependent scattering approximations are valid.

2.1. Effective medium theory

The optical properties of small particles in a medium (x<0.3) can be represented based on EMT that approximates the particles and the medium as a single homogeneous medium [10]. The effective behavior of coating while interacting with other media such as substrate and air can then be estimated based on the effective properties [15]. The effective complex dielectric function can be defined by the Maxwell Garnett approximation as

$$\varepsilon_{e,\lambda}=\varepsilon_{r,\lambda}\frac{\varepsilon_{p,\lambda}+2\varepsilon_{r,\lambda}+2f_v(\varepsilon_{p,\lambda}-\varepsilon_{r,\lambda})}{\varepsilon_{p,\lambda}+2\varepsilon_{r,\lambda}-f_v(\varepsilon_{p,\lambda}-\varepsilon_{r,\lambda})} \tag{1}$$

The resin materials are non-magnetic; therefore, the refractive and extinction indices of the coating can be represented in terms of complex dielectric function, $\varepsilon_{e,\lambda}=\varepsilon'_{e,\lambda}-i\varepsilon''_{e,\lambda}$ [31] as,

$$n_{e,\lambda}^2=\frac{1}{2}\left(\varepsilon'_{e,\lambda}+\sqrt{\varepsilon'^{\,2}_{e,\lambda}+\varepsilon''^{\,2}_{e,\lambda}}\right) \tag{2}$$

$$k_{e,\lambda}^2=\frac{1}{2}\left(-\varepsilon'_{e,\lambda}+\sqrt{\varepsilon'^{\,2}_{e,\lambda}+\varepsilon''^{\,2}_{e,\lambda}}\right) \tag{3}$$

If thickness of absorbing thin film coating on a metal substrate is larger than wavelength [15], the spectral reflectance for normal incidence can be estimated as;

$$R_\lambda=\frac{\rho_{c,\lambda}+\rho'_{c,\lambda}(1-2\rho_{c,\lambda})\exp(-8\pi\cdot t\cdot k_{e,\lambda}/\lambda)}{1-\rho_{c,\lambda}\rho'_{c,\lambda}\exp(-8\pi\cdot t\cdot k_{e,\lambda}/\lambda)} \tag{4-a}$$

otherwise, interference effects occur and spectral reflectance for normal incidence can be estimated as;

$$R_\lambda=\left|\frac{r_{c,\lambda}+r'_{c,\lambda}\exp(-4i\pi\cdot t\cdot n_{e,\lambda}/\lambda)}{1+r_{c,\lambda}r'_{c,\lambda}\exp(-4i\pi\cdot t\cdot n_{e,\lambda}/\lambda)}\right|^2 \tag{4-b}$$

where spectral reflection coefficient at air to coating boundary is

$$r_{c,\lambda}=\frac{1-(n_{e,\lambda}-ik_{e,\lambda})}{1+(n_{e,\lambda}-ik_{e,\lambda})} \tag{5}$$

and spectral reflection coefficient at coating to substrate boundary is

$$r'_{c,\lambda}=\frac{(n_{e,\lambda}-ik_{e,\lambda})-(n_{s,\lambda}-ik_{s,\lambda})}{(n_{e,\lambda}-ik_{e,\lambda})+(n_{s,\lambda}-ik_{s,\lambda})} \tag{6}$$

where n_e, n_s, are effective coating refractive index and substrate refractive index, k_e and k_s are effective coating absorption and substrate absorption index respectively.

2.2. Independent scattering: Lorenz-Mie theory

When the particles are larger, and they are distinctive, EMT is no longer valid and the radiative transfer equation must be solved. LMT defines scattering and absorption behavior of a single scattering medium consisting of spherical particles based on analytical solution of Maxwell equations [15] and it can be used to model the radiative behavior of the pigmented coatings approximating pigments as uniformly sized spheres, considering the resin material as dielectric. Formulation of the theory is described in [24, 26] with details, and it is not repeated here.

2.3. Dependent Scattering: T-matrix method

When clearance to wavelength ratio is small ($c/\lambda \leq 0.5$), effect of neighboring particles becomes significant. This effect arises from two reasons: Radiation scattered from a particle can interfere with scattered radiation from another particle (far field effect), and the internal electromagnetic field of a particle can be affected by scattering by neighboring particles (near field effect). In such a case, the radiative transfer properties must be predicted through the solution of Maxwell equations considering the neighboring particles. T-matrix method (TMM), also known as extended boundary condition method or null-field method, is a general solution method to electromagnetic field equations that is applicable to dependent or independent scattering problems of spherical or non-spherical particles. Detailed information in regards to TMM is not presented here as it is already presented elsewhere [32]. In this study, open source implementation developed by Mackowski and Mishchenko [32] is used to estimate orientation averaged scattering and absorption cross sections and the phase function of particles in the cluster. The predictions using different number of particles and orientations were presented in [16] and the recommended configuration that is shown in Figure 1 is adopted in this study.

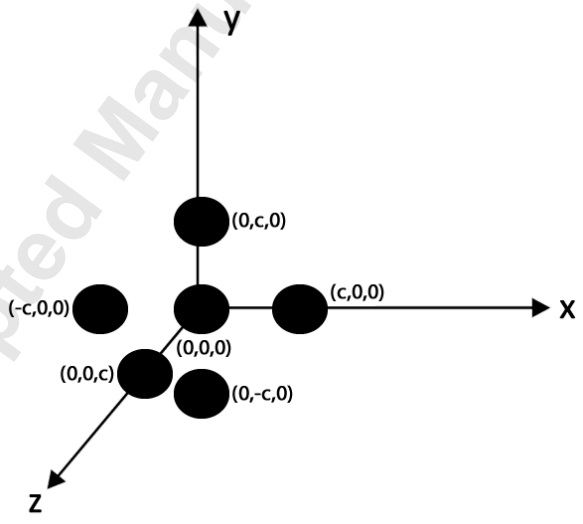

Figure 1 Pigment distribution [16] that is used to model dependent scattering.

2.4. Radiative Transfer Model of Pigmented Coatings with Four Flux Method

The pigmented coating applied on a metal substrate can be considered as a thin slab as shown in Fig. 2 that is illuminated from one side. For small particles with respect to wavelength, where effective medium approximation is valid, the absorption behavior of the coating can be estimated through Fresnel formalism (Eq. 4). For larger particles, the radiative transfer equation must be solved considering the radiative transport properties based on independent or dependent scattering. There are different methods that can be used for solution of radiative transfer equation for the one dimensional thin slab problems shown in Fig. 2. For solar collectors, the incident light have diffuse and collimated component; therefore, using four flux method is more appropriate. The FFM considers four intensities traveling through the slab as shown in Fig. 2 [13,14], where I_d is the diffuse forward, J_d is the diffuse backward, I_c is the collimated forward, and J_c is the collimated backward intensity. Through the solution of coupled differential equations written for each intensity component, the diffuse, $R_{d,\lambda}$, and collimated reflectances, $R_{c,\lambda}$, can be estimated, yielding spectral reflectance, R_λ, as:

$$R_\lambda = R_{d,\lambda} + R_{c,\lambda} \tag{7}$$

The four coupled differential equations and their solution are presented in detail in [13,14,23]. Once the spectral reflectance is calculated, spectral emittance and absorptance can be defined as:

$$\alpha_\lambda = 1 - R_\lambda \tag{8}$$

$$\epsilon_\lambda = \alpha_\lambda \tag{9}$$

Therefore, through the solution of FFM, for radiative transport properties defined by LMT or TMM, the spectral emittance of the coating can be defined based on pigment radius, volume fraction, thickness, optical properties and resin thickness.

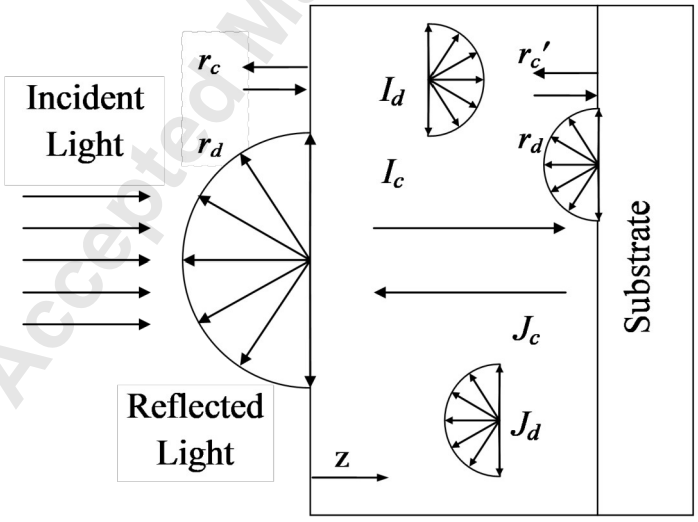

Figure 2 Sketch of the spectrally selective coating on a substrate.

A global search algorithm is to be used in this study, and a unified model (UM) is developed so that for a given set of parameters, the proper method (EMT or FFM with LMT-EHT or FFM with TMM) can be used according to the scattering regime map, as discussed earlier. Moreover, a simplified version of unified model (SUM) is developed, where only EMT and independent scattering regimes (FFM with LMT) are considered, whereas dependent scattering is ignored and LMT-EHT is used within this region instead of TMM. Coatings optimized with UM will be compared to those optimized by SUM in order to observe the effect of considering dependent scattering in optimization. A list of the models, their validity ranges and limitations are provided in Table 1.

The spectral reflectance of a coating with 400 nm PbS pigment 40% by volume in 2 μm thick polybinder is presented in Fig. 3. It can be observed that prediction of UM is identical to that of LMT-EHT in the first region ($\lambda<0.8$ μm), TMM in the second region ($0.8<\lambda<8.2$ μm) and EMT in the last region ($\lambda>8.2$ μm). Whereas, prediction of SUM is identical to that of LMT-EHT in the first two regions ($\lambda<8.2$ μm), and EMT in the last region ($\lambda>8.2$ μm). Prediction of UM and SUM are presented along with the estimations of all models for the entire spectrum and it was observed that there is a good agreement at model transitions. It can also be observed that estimation of different models at each region differs. Therefore, it can clearly be observed that the estimates by using a single model along the whole spectrum will yield erroneous results.

Table 1 Validity ranges and limitations of different models used for solving radiative transfer equations and its parameters.

Methods to Estimate Scattering Phase Function, Absorption Coefficient and Scattering Coefficient			
Method name	**Validity**	**Handled Scattering Type**	
Lorentz Mie Theory (LMT)	Single sphere	Single Scattering	
T-Matrix Method (TMM)	Single / Cloud of spheres	Single / Multiple Scattering	
Methods to Implement Multiple Scattering to LMT			
Method Name	**Validity**		
Hartel Theory	Optically thin medium		
Extended Hartel Theory (EHT)	Optically thick and thin medium		
Methods to Estimate Reflectance			
Method Name	**Scattering Type**	**Valid For Size Parameter**	**Valid For Particle Clearance Wavelength Ratio**
Four-Flux Method (FFM) with LMT - EHT	Independent multiple	$x>0.3$	$c/\lambda>0.5$
Four-Flux Method (FFM) with TMM	Dependent multiple	$x>0.3$	$c/\lambda \leq 0.5$
Effective Medium Theory (EMT)	No scattering	$x \leq 0.3$	Particles are indistinguishable

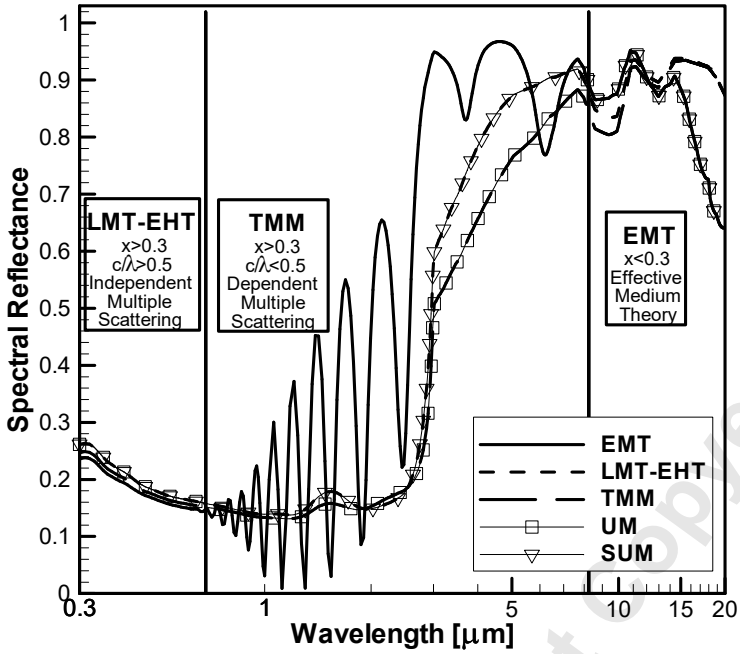

Figure 3 Spectral reflectance for different regimes of unified model.

3. Problem Statement and Formulation

The net heat transferred to the working fluid must be maximized in order to maximize the performance of a solar thermal system. The radiation incident to the absorber of a generic system can be defined in terms of solar irradiation and a concentration factor, C_f, which is 1 for flat plate collectors and larger than 1 for concentrating collectors. For a given absorber temperature, concentration factor, coating properties the net heat transfer can be formulated as:

$$q'' = \int_0^\infty \left[\alpha_\lambda G_{s,\lambda} C_f - \epsilon_\lambda E_{b,\lambda}(T_a)\right] d\lambda \tag{10}$$

Considering that $\alpha_\lambda = \epsilon_\lambda$, and dominant emission wavelengths of sun and absorber, the spectral emittance of an ideal solar coating that maximizes the net heat flux can be represented as:

$$\epsilon_{\text{ideal},\lambda} = \begin{cases} 1 & \lambda \le \lambda_c \\ 0 & \lambda > \lambda_c \end{cases} \tag{11}$$

where λ_c represents a cut-off wavelength that depends on the absorber temperature, T_a, concentration factor, C_f, and solar irradiation $G_{s,\lambda}$. For a given set of T_a, C_f and $G_{s,\lambda}$, λ_c can be identified by maximizing net heat flux as explained in [24]. In this study, standard solar radiation based on ASTM-G-173-3 [33] is considered and corresponding λ_c values for given set of T_a, C_f are presented in Table 2.

The design problem is considered as an inverse problem of predicting the cause of a desired behavior. Since ideal coating yields the maximum net absorber radiant heat flux, the objective function to be minimized can be formulated so that the parameters yielding similar or identical performances with that of the ideal coating

$$F(\chi)=\int_0^\infty \{[G_{s,\lambda}C_f - E_{b,\lambda}(T_a)][\epsilon_{ideal,\lambda}-\epsilon_\lambda(\chi)]\}d\lambda \quad (12)$$

where χ represents the set of parameters to be identified, $[r_p\ f_v\ t]^T$.

Considering the non-linearity of spectral emittance of the pigmented coating, a direct solution for minimization of Eq. (12) is not possible. Optimization is used for solution non-linear inverse design problem similar to [28, 29].

There are various pigments used in spectrally selective solar coatings such as, nickel, germanium, carbon, silicon, copper dioxide, lead sulfide which are tabulated in [26]. Achieving high solar absorptance is possible by using dark colored or black pigments with relatively higher extinction index such as nickel (Ni), lead sulfide (PbS) and carbon (C). Therefore, these three pigments are considered for the optimization study along with the polybinder. Refractive index for these pigments and binder are available in [26] and [34], respectively, and is not presented here.

A maximum volume fraction of 0.52 is experimentally observed in [35]. Thus, upper limit for volume fraction is selected as 0.5, which is also the upper limit for Maxwell-Garnett Effective Medium theory. Gunde and Orel [30] defines minimum clearance between particles as:

$$c=\frac{x\lambda}{\pi}\left(\frac{0.905-f^{1/3}}{f^{1/3}}\right) \quad (13)$$

Etherden *et al.* [26] suggested that pigment size should be substantially smaller than the film thickness. A constraint is introduced to ensure that coating thickness is greater than 5 radii, As a result, single layer pigment structure is avoided and FFM is applicable at all cases. Pigments with radii as low as 20 nm is reported in [35], which is considered as the lower limit for radius in this study. Similarly, 0.3 μm coating thickness is reported in [7] for pigmented coatings, and this thickness is considered as the lower limit for thickness.

Carbon element is stable up to 1023 K, whereas PbS particles are stable up to 400 K [36] and 100% silicone binder can be stable up to 800 K [37]. Considering the material properties, medium temperature and high-temperature absorber cases are considered as 373K and 773 K, respectively. For concentrating collector cases, C_f is considered as 30 and 60, which are within the practical range suggested by literature [38].

4. Optimization Method

The minimization of the objective function described by Eq. (12) is a non-linear optimization problem and the system has a complex topology with multiple local extrema. Therefore, use of gradient based methods could yield solutions dependent on the initial guess and global search algorithms must be used to overcome this problem. Simulated annealing (SA) is one

of the most widely used global search algorithms due to its high performance and wide applicability [39].

The method mimics the physical process of annealing of solids [40]. It starts with an initial guess, $\chi_0=[r_{p,0}\ f_{v,0}\ t_0]^T$, that is considered as the current point and an initial temperature, $T_o=100$. At every step, temperature is decreased based on, $T=0.95^k T_o$, where k is the iteration number. A random candidate point $\chi_{cp}=[r_{p,cp}\ f_{v,cp}\ t_{cp}]^T$ is created in a random direction, with a step length T from the current point. If the value of the objective function at the candidate point, $F(\chi_{cp})$ is smaller than that of the current point, $F(\chi_k)$, the candidate point replaces the current point as $\chi_{k+1}=\chi_{cp}$. Otherwise the acceptance of the candidate point is randomly evaluated based on a probability distribution function representing the annealing process as:

$$P=\frac{2}{1+\exp\left(\frac{\Delta F}{T}\right)} \tag{14}$$

Here P is the probability of acceptance, ΔF is difference between current value of the objective function and previous one. If P is smaller than a generated pseudo random number, then candidate point is accepted although the current solution is better, which resembles the candidate point proceeding through a local minimum. If P is not smaller than the generated pseudo number, then a new random candidate point χ_{cp} is created. At first iterations, where the temperature is high, possibility of selecting worse candidate point is high; therefore, method can check values from different local minimums. As temperature decreases, method converges near the global minimum.

Metaheuristic methods such as SA execute more objective function evaluations than gradient based optimization methods such as Newton or Quasi Newton method. However, SA is capable of handling discontinuous and multiple extremum systems. While Genetic Algorithm is another widely used global optimization method, it was reported in [41] that SA has higher convergence than genetic algorithm. Thus, SA is used in this study due to its robustness and ease of applicability [42]. More detailed information about SA is available in literature [43].

5. Results and Discussion

This study considers inverse design of spectrally selective pigmented coatings to maximize the energy harvesting from sun for solar-thermal applications. Integrated form of Eq. (12), represents net heat flux when all convection loses are ignored and can be presented as

$$q''=\alpha_s C_f G_s-\epsilon\sigma T_a^4 \tag{15}$$

where α_s is the solar absorptance, ϵ is the total emittance of the coating, and G_s is the total solar irradiance. In order to maximize the net heat flux received by absorber, high solar absorptance is desired along with low total emittance.

5.1. Model Validation and Verification

Verification and validation studies are performed to understand the predictive accuracy of the UM before using it for design of pigmented coatings. The verification of the UM for dependent and independent scattering regime is performed by comparing predicted results with those in [16] and represented in Fig. 4. Predictions show good agreement with data from literature for both LMT-EHT and TMM. Besides, significant difference is observed between estimations of spectral reflectance considering dependent and independent scattering approximations from 1μm to 2 μm, which implies that predictions by LMT-EHT are not accurate within this band. The model is further validated for small size parameters where EMT is valid and the predictions are presented in Fig. 4 together with experimental data from literature [25]. The comparisons presented indicate that the UM is in good agreement with measured and calculated values, thus validating the model. However, predictions of SUM that ignores dependent scattering, diverge from those of UM within this regime as expected.

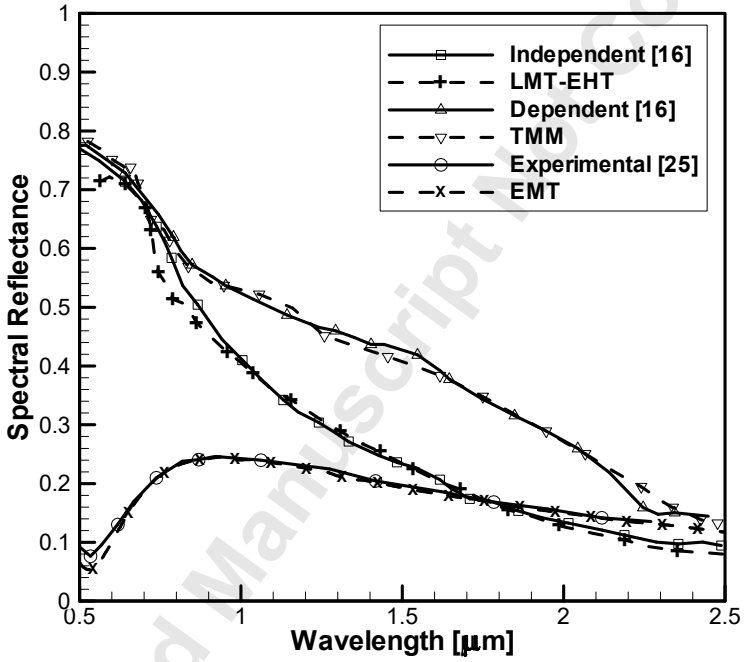

Figure 4 Spectral reflectance vs wavelength for validation and verification studies.

5.2. Demonstration of SA

The optimal coating leading to maximum net heat transfer is identified by inverse design by minimizing the objective function presented in Eq. (12). In order to demonstrate inverse design's capability of finding optimum coating leading to maximum heat flux, a design problem is considered with PbS pigment in polybinder, for an absorber at 373 K and C_f=1. The contour plots of net heat flux change with r_p and t, for three discrete f_v values (f_v = 0.1, 0.2 and 0.3) are presented in Figs. 5-(a-d), respectively. It can be observed that the system has multiple local extrema and SA is capable of identifying the global maximum, by minimizing the objective function presented in Eq. (12). The iteration points initially populating around

Journal of Solar Energy Engineering. Received August 02, 2017;
Accepted manuscript posted February 08, 2018. doi:10.1115/1.4039276

the local minima, populates to global maximum more densely as iterations proceed and at the end the algorithm converge to global maximum.

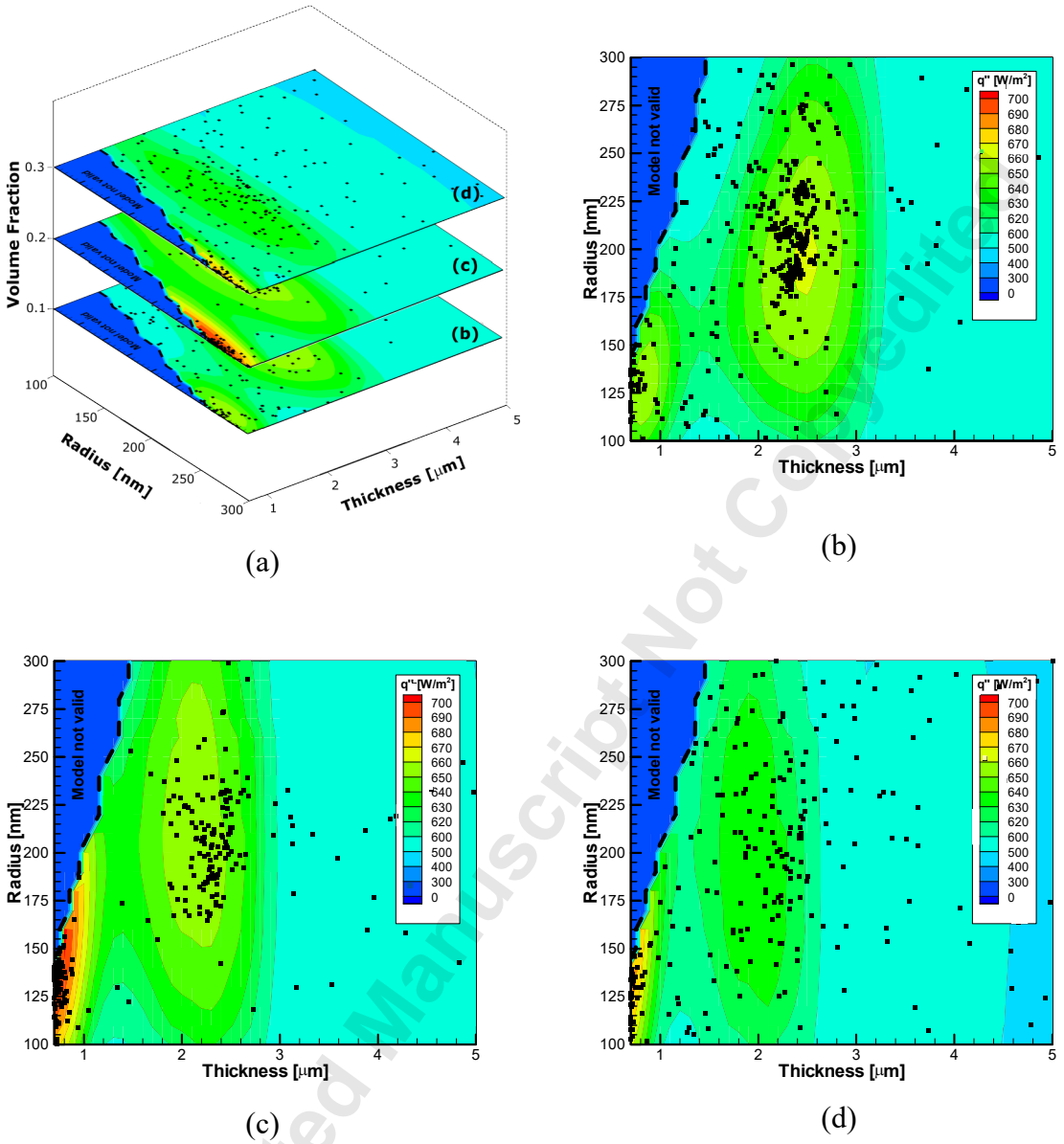

Figure 5 SA iterations and variation of net heat flux for (a)f_v=0.1,0.2,0.3 together, (b) f_v=0.1, (c) f_v=0.2, and (d) f_v=0.3.

5.3. Evaluation of Different Pigments

Solution of the design problem using objective function defined by Eq. (12), for three different pigments, C, Ni and PbS, are carried out for different concentration factors and absorber temperatures by using UM and SA algorithm. A summary of the results are presented in Table 2, where it can be observed that the total solar absorptance of PbS and carbon pigmented coatings are similar, whereas Ni pigmented coatings has a lower absorptance for an absorber temperature of 373 K. Moreover, total emittance of carbon pigmented coating is larger than that of PbS and nickel pigmented coatings. Besides, the

coating with PbS pigments follows the behavior of the ideal coating more closely than carbon and nickel (Fig. 6). Therefore, PbS appears to be a more suitable pigment material for the flat plate problem, with carbon pigmented coating has excessive heat loss due to higher emission, and nickel pigmented coating results has lower absorption.

Table 2 Summary of optimal parameters for spectrally selective coatings for solar thermal systems.

T_a [K]	Pigment	C_f	r_p [nm]	f_v	t [μm]	α_s	ϵ	q'' [kW/m^2]	λ_c [μm]
373	PbS	1	142	0.21	0.7	0.85	0.05	0.72	2.51
	Ni	1	110	0.18	0.6	0.80	0.05	0.67	2.51
	C	1	130	0.3	0.7	0.84	0.10	0.65	2.51
773	C	30	163	0.11	2.1	0.89	0.23	19.48	2.31
	C	60	163	0.11	2.9	0.91	0.27	43.96	2.40

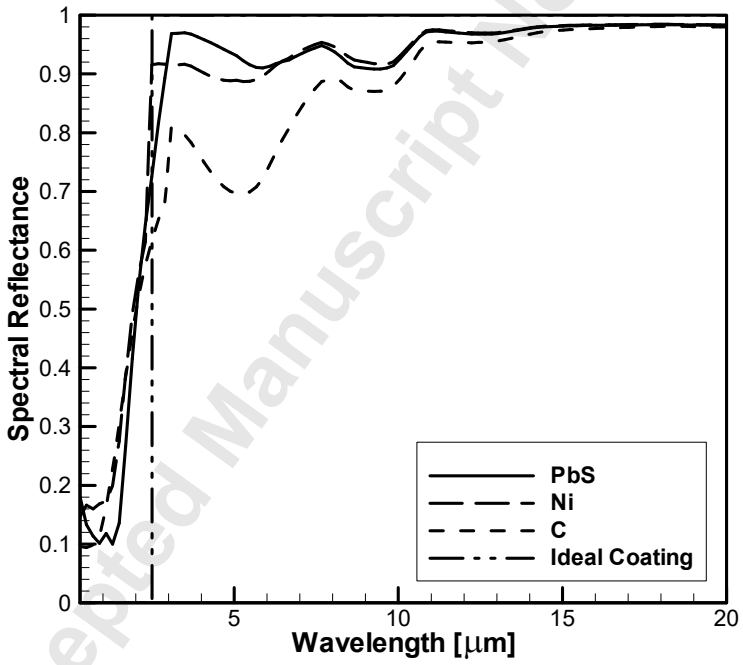

Figure 6 Optimal spectral emittance of different materials at T_a=373 K, C_f=1

Although pigmented coatings are mostly preferred for low cost applications, where temperatures are relatively low, the study also considers high temperature cases to further identify the behavior of pigmented coatings. Using PbS pigmented coatings for high temperature applications is not possible due to their instability at higher temperatures. Moreover, as carbon pigmented coatings has higher absorptance than nickel pigmented ones, and their relatively high emissivity has less significant effect as concentration factor increases, only carbon pigmented coatings are considered for high temperature applications. The total and spectral emittance of the carbon pigmented coatings for C_f of 1, 30 and 60 are

presented in Table 2 and Fig. 7, respectively. It can be observed hat, as concentration factor increases, the optimal coating's total emittance and solar absorptance both increase. However, emittance becomes less significant and increasing absorptance dominates with increasing concentration factor.

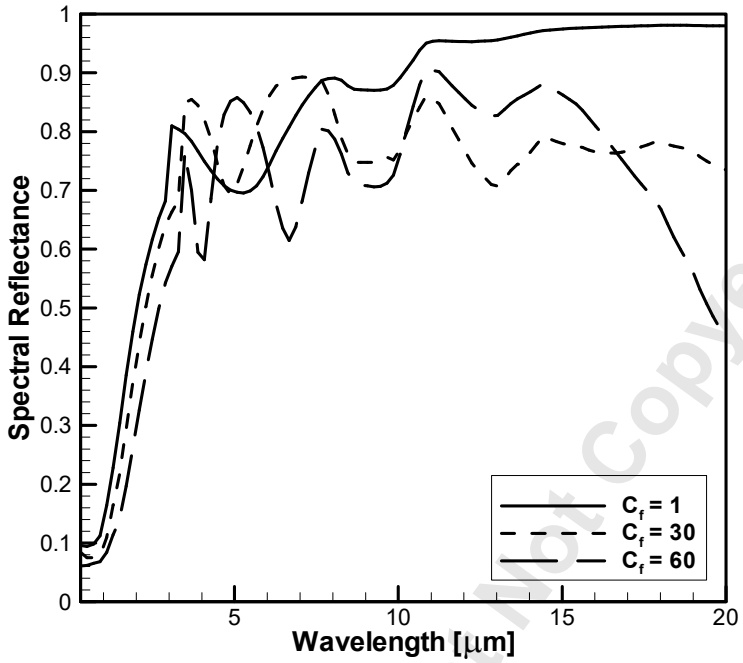

Figure 7 Comparison of spectral reflectance of the optimal pigmented coatings with carbon pigments for flat plate, and two concentrating solar collectors.

Etherden *et al.* [25] suggested that optimal radii for pigmented coatings are around 100 nm and they also claimed if further optimization study is carried out the exact optimum radii could be found between 100 and 200 nm, for Ni, C and PbS pigmented coatings and different absorber temperatures. The optimal radii estimated in this study are in agreement with their suggested range as presented in Table 2.

5.4. Parametric Analysis:

Parametric analysis is carried out next to identify the effect of each design variable on collection efficiency. Here the collection efficiency is defined as;

$$\eta_c = \frac{q''_{net}}{G_s C_f} \tag{16}$$

and it represents the ratio of net absorber radiant heat flux to solar irradiation. The parametric analysis considers the optimal coating parameters presented in Table 2, varying one parameter at a time, keeping the other two constant. The effect of coating thickness on collection efficiency is presented in Fig. 8. Absorptance and emittance increases with increasing thickness. Increase of emittance dominates increase of absorptance after optimum point, thus efficiency starts to decrease. Oscillatory behavior of the decrease is due to interference effect modeled by EMT, which is discussed in detail by Laaksonen *et.al.* [44]. A

number of local extrema can be observed aside from the global extremum that justifies the use of global search algorithms. Oscillation effect in emittance due to interference is more noticeable than reflectance as longer wavelengths results a lower coating thickness to wavelength ratio. Therefore the oscillation is more prevailing for flat plate collectors than concentrated collectors..

FFM with LMT - EHT and FFM with TMM use scattering and absorption coefficients to estimate reflectance. Etherden *et.al.* [26] states particle size is crucial for scattering and absorption coefficients and an optimization study that considers radii between 100 and 500 nm will reveal exact optimal particle for different pigments. Fig. 9. shows that pigments has optimum radius values that meets with predictions of Etherden *et.al.* [26]. From Fig. 9, it can be observed that the particle size have a limited effect on collection efficiency for carbon. However, it appears to be critical for nickel pigments. Considering that the pigments have a size distribution, ignoring the size distribution will not have any significant effect on carbon pigments, whereas a narrow distribution is desired for nickel.

The effect of pigment volume fraction is presented in Fig. 10, where a significant variation in collection efficiency is observed with changing pigment volume fraction. Absorptance and emittance increases with increasing volume fraction, after optimum volume fraction; increase of emittance dominates increase of absorptance and efficiency starts to decrease. This effect is more pronounced at higher concentration ratios, where the optimal particle volume fraction is lower.

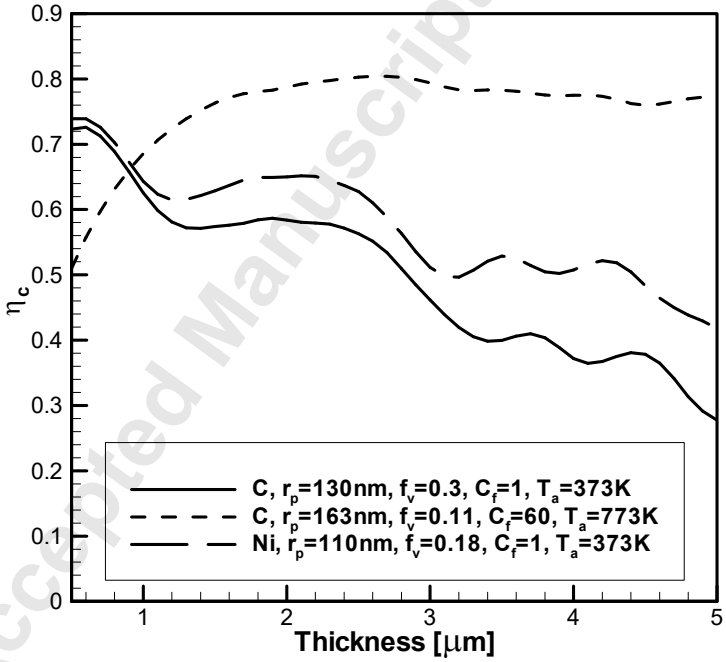

Figure 8 Variation of collection efficiency with thickness.

Journal of Solar Energy Engineering. Received August 02, 2017;
Accepted manuscript posted February 08, 2018. doi:10.1115/1.4039276

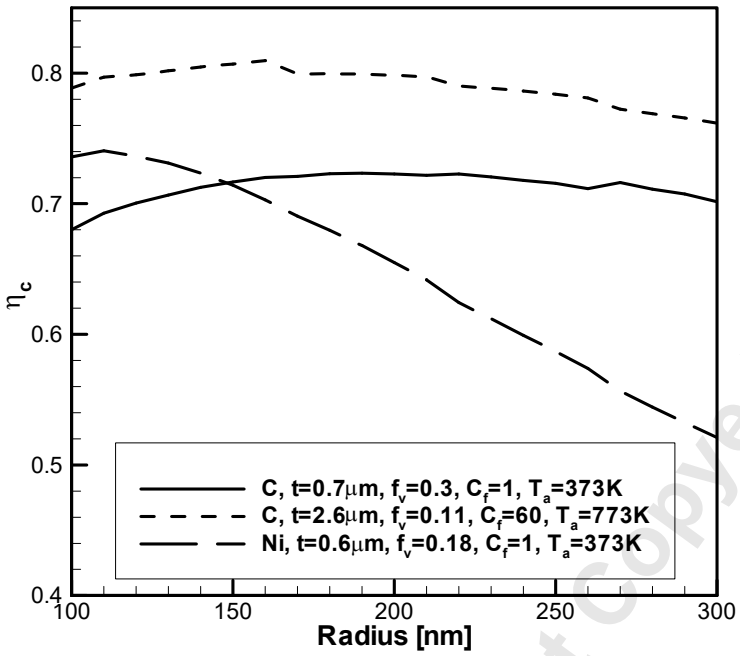

Figure 9 Variation of collection efficiency with radius.

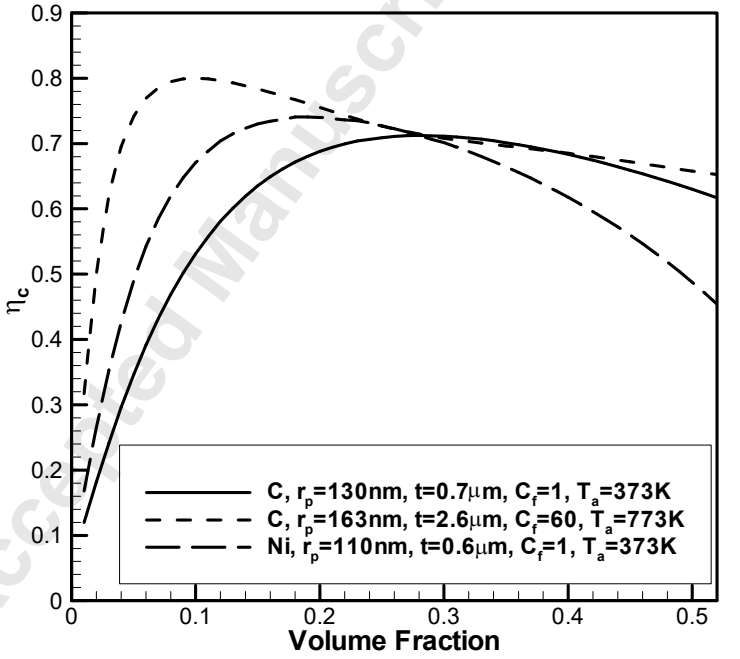

Figure 10 Variation of collection efficiency with volume fraction.

5.5. Evaluation of Different Models

Most of the prior studies rely on a single model such as EMT or LMT over entire variable domain [25, 26]. In this study, unified models are developed and verified for designing pigmented coatings to overcome the limitations in regards to each model. In an additional study, use of EMT, LMT-EHT, UM and its simplified version SUM is evaluated for such an optimization by considering resulting collector efficiency and required computation time. This is accomplished by designing 4 coatings using EMT, LMT-EHT, SUM and UM for a prescribed case, and predicting the performance of the 4 identified coating parameters using UM that is the most accurate model.

Design of PbS and carbon pigmented coatings are performed for flat a plate collector at 373K, and for a parabolic collector at 773 K, respectively. Optimized design variables (r_p, f_v, t) and the corresponding performance parameters (α_s, ϵ, q'', η_c) predicted by each model compared to the expected values predicted by UM are presented in Tables 3 and 4. For flat plate, the coating designed by using EMT is 11% less efficient than the one that is optimized by using UM as seen in Table 3. The coating designed by EMT has a higher emittance than the coating designed by UM, which is more critical for a flat plate collector. However, the predicted emittances are similar for EMT and UM, as the absorber emits mostly in longer wavelengths where the size parameter is low and UM uses EMT. Although using LMT-EHT yields a coating design with relatively higher solar absorptance (α_s=0.92), the resulting efficiency is 19% lower due to the high emittance (ϵ=0.25) of the coating. LMT-EHT is not capable of accurately predicting the emittance at these wavelengths, predicting emittance as 0.04 that is significantly different from the prediction by UM leading to a poorly performing design. However, using SUM and UM yield almost identical designs and performances (α_s=0.85 and ϵ=0.05).

As it can be seen in Table 4, the coating designed by using EMT is 4.2% less efficient than the one that is designed by using UM, for concentrating collector. Considering the high concentration factor, the maximizing the absorptance is more critical than minimizing the emittance for this case. Therefore, using carbon pigments leads to a coating with relatively higher solar absorptance and emittance (α_s=0.90 and ϵ=0.35). Using LMT-EHT yields a slightly better coating design than that by using EMT in this particular case where emittance is less significant. Similar to the previous case, using SUM and UM yield identical designs and performances (α_s=0.91 and ϵ=0.27).

Results indicate that SUM can be used to optimize pigmented solar coatings. Coating designed by LMT-EHT performs weakly for flat plate applications due to high total emittance as presented in Table 3. Effect of total emittance becomes less significant for concentrating collectors; therefore, using LMT-EHT results in more accurate predictions for concentrating collector applications as presented in Table 4.

Computation time required for estimation of total reflectance using each model is presented in Table 5. While TMM is the most expensive method due to increased matrix size based on number of spheres considered in the estimation of extinction and scattering efficiencies, UM reduces computation time by 95% with respect to solely using TMM. Considering that the optimization algorithm performs about 1500-2500 total reflectance estimations depending on initial guess and coating properties. For TMM, the optimization takes about 50 days, and UM requires approximately two and a half days of computation. However, using SUM provides further significant improvement and design can be completed within minutes.

Therefore, SUM is suggested as a good compromise between accuracy and computational efficiency.

Table 3 Optimized design variables (r_p, f_v, t) and the corresponding performance parameters (α_s, ϵ, q'', η_c) predicted by each model compared to the expected values predicted by UM for PbS pigmented coating at T=373K

Model	r_p [nm]	f_v	t [μm]	*Model* α_s	ϵ	q'' [W/m^2]	η_c [%]	*UM* α_s	ϵ	q'' [W/m^2]	η_c [%]
EMT	20	0.32	2.4	0.86	0.15	619	68.4	0.87	0.15	619	68.4
LMT-EHT	192	0.05	4.9	0.92	0.04	777	86.0	0.92	0.25	550	60.8
SUM	140	0.20	0.7	0.85	0.05	709	78.4	0.85	0.05	717	79.3
UM	142	0.21	0.7	-	-	-	-	0.85	0.05	718	79.4

Table 4 Optimized design variables (r_p, f_v, t) and the corresponding performance parameters (α_s, ϵ, q'', η_c) predicted by each model compared to the expected values predicted by UM for C pigmented coating for C_f=60 at T=773K

Model	r_p [nm]	f_v	t [μm]	*Model* α_s	ϵ	q'' [kW/m^2]	η_c *(%)*	*UM* α_s	ϵ	q'' [kW/m^2]	η_c *(%)*
EMT	20	0.26	1.7	0.90	0.35	41.9	77.0	0.90	0.35	41.7	76.9
LMT-EHT	180	0.03	9.9	0.91	0.25	44.3	81.7	0.92	0.34	42.1	77.6
SUM	163	0.11	2.9	0.91	0.26	43.9	80.9	0.91	0.27	43.9	80.9
UM	163	0.11	2.9	-	-	-	-	0.91	0.27	44.0	81.1

Table 5 Computation time of calculating objective function with TMM, EMT, LMT- EHT and unified models separately for PbS pigment. r_p=170 nm, f_v=0.2, t=1 μm on single core of 3.40 GHz CPU.

Method	CPU Time (seconds)
EMT	0.2
LMT-EHT	0.5
TMM	2437
SUM	0.4
UM	123

6. Conclusions

Inverse design of spectrally selective pigmented coatings is proposed for solar thermal systems. A unified model and simplified unified model are developed, for predicting the radiative transport properties of pigmented coatings. In these models, Lorenz-Mie theory in conjunction with extended Hartel theory is used to predict radiative properties for independent scattering with multiple scattering effects, whereas T-matrix method is used for dependent scattering for unified model, along with effective medium theory for very small pigments. While T-matrix is a precise model, it requires significant computation time; therefore, for simplified unified model, T-matrix method is not used ignoring dependent scattering effects. Once the radiative transport properties are estimated, the spectral emittance of the coating is calculated by four flux method. It is observed that the simplified unified model is capable of designing and modeling coatings adequately and can be considered as a good compromise between efficiency and accuracy.

Ideal coating behavior depends on working conditions of the system such as absorber temperature, and concentration factor. The design problem can be formulated as estimating the design parameters, for achieving the ideal coating behavior. Such a design problem can be considered as an inverse problem, where a system that exhibits a desired behavior under known conditions is predicted. Moreover, the design problem is a non-linear inverse problem due to highly non-linear dependence of coating behavior on design parameters. Therefore, the solution of the non-linear inverse design problem is achieved through optimization techniques. The optimization problem is formulated as a minimization problem of an objective function and solution by gradient based algorithms is highly dependent on initial guess due to existing multiple local extrema. Therefore, global search algorithms must be used. Simulated Annealing algorithm is used in this study that successfully locates global minimum independent of initial condition.

It was found that the net solar absorptance of coatings with lead sulfide pigments is superior to carbon and nickel pigments for medium temperature applications. While the solar absorptance of lead sulfide pigmented coating is similar to that of carbon pigments, it has significantly lower total emittance. Therefore, the net heat flux for absorber with lead sulfide pigmented coatings is larger. However, as lead sulfide is unstable at high temperatures and nickel has lower absorptance, carbon pigment is used for high temperature applications where it shows better performance with respect to medium temperature. The optimal pigment radius, coating thickness and volume fraction is dependent on prescribed absorber temperature and concentration factor. Therefore, it was shown that pigmented coatings must be designed considering the operating conditions of the system.

Based on this study, it can be concluded that inverse design is a useful tool that can be applied for solution of design problems in different energy systems. The design method presented in this study is flexible and by modifying the objective function, different constraints and considerations can be easily incorporated to the design problem.

7. Acknowledgements

The authors would like to thank the Boğaziçi University, for support under B.U. Research Fund AP-5566P.

8. References

1. Kalogirou S. A., 2003, "Solar Thermal Collectors and Applications," Progress in Energy and Combustion Science, 30, pp. 231-295.
2. Mar H. Y. B., Lin J. H., Zimmer P. P., Peterson R. E., and Gross J. S., 1975, "Optical Coatings for Flat Plate Solar Collectors", Report to ERDA under contract No. NSF-C-957.
3. Kennedy C. E., 2002, "Review of Mid to High Temperature Solar Selective Absorber Materials", Technical Report, NREL/TP-520-31267.
4. Duffie J. A., and Beckman W. A., 2006, Solar Engineering Of Thermal Processes. Hoboken: Wiley.
5. Peterson R. E., and Ramsey J. W., 1975, "Thin Film Coatings in Solar Thermal Power Systems," Journal of Vacuum Science and Technology, 12, pp. 174-181.
6. Orel B., Radoczy I., and Orel Z. C., 1986, "Organic Soot Pigmented Paint for Solar Panels: Formulation, Optical Properties and Industrial Application," Solar & Wind Technology, 3, pp. 45-52.
7. Gunde M. K., Logar J. K., Orel Z. C., and Orel B., 1996, "Optimum Thickness Determination To Maximize The Spectral Selectivity Of Black Pigmented Coatings For Solar Collectors", Thin Solid Films, 277, pp. 185-191.
8. Orel Z. C., and Gunde M. K., 2001, "Spectrally Selective Paint Coatings: Preparation and Characterization.", Solar Energy Materials and Solar Cells, 68, pp. 337-353.
9. Granqvist C. G., 1985, "Spectrally Selective Coatings for Energy Efficiency and Solar Applications," Physica Scripta, 42, pp. 401-407.
10. Niklasson G. A., 2006, "Modeling The Optical Properties of Nano-Particles," SPIE Newsroom.
11. Vargas W. E., and Niklasson G. A., 1997, "Applicability Conditions of The Kubelka-Munk Theory.", Applied Optics, 36, pp. 5580-5586.
12. Vargas W. E., and Niklasson G. A., 1997, "Generalized Method for Evaluating Scattering Parameters Used in Radiative Transfer Models," Journal of Optical Society of America, 14, pp. 2243-2252.
13. Maheu B., Letoulouzan J. N., and Gouesbet G., 1984, "Four-Flux Models To Solve The Scattering Transfer Equation In Terms Of Lorentz-Mie Parameters," Applied Optics, 23, pp. 3353-3362.
14. Vargas W. E., 1998, "Generalized Four-Flux Radiative Transfer Model." Applied Optics, 37, pp. 2615-2623.
15. Howell J. R., Mengüç M. P., and Siegel R., 2015, Thermal Radiation Heat Transfer. 6th ed. Boca Raton: CRC Press.
16. Vargas W.E., 2003, "Optical Properties Of Pigmented Coatings Taking Into Account Particle Interactions." Journal of Quantitative Spectroscopy and Radiative Transfer, 78, pp. 187-195.
17. Vargas W.E., Lushiku E. M., Niklasson G. A., and Nilsson T. M. J., 1998, "Light Scattering Coatings: Theory And Solar Applications.", Solar Energy Materials and Solar Cells, 54, pp. 343-350.
18. Vargas W.E., and Niklasson G. A., 2001, "Reflectance Of Pigmented Polymer Coatings: Comparisons Between Measurements And Radiative Transfer Calculations.", Applied Optics, 20, pp. 85-94.
19. Vargas W. E., Greenwood P., Otterstedt J. E., and Niklasson G. A., 2000, "Light Scattering In Pigmented Coatings: Experiments And Theory," Solar Energy, 68, pp. 553-561.

20. Vargas W. E., 2000, "Optimization Of Diffuse Reflectance Of Pigmented Coatings Taking Into Account Multiple Scattering," Journal of Applied Physics, 88, pp. 4079-4084.
21. Baneshi M, Maruyama S, Nakai H, and Komiya A., 2009, "A New Approach To Optimizing Pigmented Coatings Considering Both Thermal And Aestetic Effects," Journal of Quantitative Spectroscopy and Radiative Transfer, 110, pp. 192-204.
22. Baneshi M, Maruyama S, and Komiya A., 2011, "Comparison Between Aesthetic And Thermal Performances Of Copper Oxide And Titanium Dioxide Nano-Particulate Coatings." Journal of Quantitative Spectroscopy and Radiative Transfer, 112, pp. 1197-1204.
23. Gonome H., Baneshi M., Okajimac J., Komiyac A., and Maruyama S., 2014, "Controlling The Radiative Properties Of Cool Black-Color Coatings Pigmented With CuO Submicron Particles.", Journal of Quantitative Spectroscopy and Radiative Transfer, 132, pp. 90-98.
24. Yalcin R. A., and Erturk H., 2011, "Optimization of Pigmented Coatings for Concentrating Solar Thermal Systems", Proceedings of 2011 International Mechanical Engineering Congress and Exhibition, Denver, Co, USA, November 11-17, 2011.
25. Zhao S., and Wackelgard E., 2006, "Optimization Of Solar Absorbing Three-Layer Coatings," Solar Energy Materials & Solar Cells, 90, pp. 243–261.
26. Etherden N, Tesfamichael T, Niklasson GA, and Wackelgård E., 2004, "A Theoretical Feasibility Study Of Pigments For Thickness-Sensitive Spectrally Selective Paints," Journal of Physics D: Applied Physics, 37, pp. 1115-1122.
27. Gonome H, Okajima J, Komiya A, and Maruyama S., 2014, "Experimental Evaluation Of Optimization Method For Developing Ultraviolet Barrier Coatings," Journal of Quantitative Spectroscopy and Radiative Transfer, 133, pp. 454-463.
28. Howell J. R., Daun K. J., Erturk H., Gamba M., and Hosseini S. M., 2003, "The Use Of Inverse Methods For The Design And Control Of Radiant Sources." JSME International Journal, Series B, Fluid and Thermal Engineering, 46, pp. 470-478.
29. Daun K. J., Erturk H., and Howell J. R., 2002, "Inverse Methods For High Temperature Systems.", Arabian Journal for Science and Engineering, 27, pp. 3-48.
30. Brewster M. Q., and Tien C. L., 1982, "Radiative Transfer In Packed Fluidized Beds: Dependent Versus Independent Scattering". Journal of Heat Transfer, 104, pp. 573-579.
31. Modest M. F., 2003, Radiative Heat Transfer. 2nd ed. Boston: Academic Press.
32. Mackowski D. W., and Mishchenko M. I., 2011, "A Multiple Sphere T-Matrix Fortran Code For Use On Parallel Computer Clusters". Journal of Quantitative Spectroscopy and Radiative Transfer, 112, pp. 2182-2192.
33. American Society for Testing and Materials (ASTM) Terrestrial Reference Spectra, ASTM G-173-03.
34. Kunitomo T., Tsuboi Y., Iwashita S., and Shafey H.M., 1983, "Theoretical Study on Spectrally Selective Paint Coatings," Solar World Congress, 3, pp. 1943-1947.
35. Tesfamichael T., Hoel A., Wäckelgård E., Niklasson G., Gunde M., and Orel Z., 2001, "Optical Characterization And Modeling Of Black Pigments Used In Thickness Sensitive Solar Selective Absorbing Paints," Solar Energy, 69, pp. 35-43.
36. Sadovnikov SI, Kozhevnikova NS, and Rempel AA., 2011, "Stability And Recrystallization Of Pbs Nanoparticles," Inorganic Materials, 47(8), pp. 837-843.
37. Gordon J., Solar Energy: The State of the Art: ISES Position Papers, p. 121.
38. Meinecke W. Renewable Energy Systems And Desalination. Vol. II - Parabolic Trough Collectors
39. Avriel M., 2003, Nonlinear Programming Analysis And Methods. New York: Dover.
40. Kirkpatrick S., Gelatt C. D., and Vecchi M. P., 1983, "Optimization by Simulated Annealing", Science, 220, pp. 671-680.

41. Lahtinen J., Myllymaki P., Silander T., and Tirri H., 1996, "Empirical Comparison Of Stochastic Algorithms", Proceedings of the Second Nordic Workshop on Genetic Algorithms and their Applications, Vaasa, Finland, August 1996, pp. 45-59.
42. Porter J. M., Larsen M. E., Barnes J. W., and Howell J. R.,2006, "Metaheuristic Optimization Of A Discrete Array Of Radiant Heaters," Journal of Heat Transfer, 10, pp. 1031-1040.
43. Bertsimas D., and Tsitsiklis J., 1993, "Simulated Annealing," Statistical Science, 8, pp. 10-15.
44. Laaksonen K., Li S.-Y., Puisto S.R., Rostedt N.K.J., Ala-Nissila T., Granqvist C.G., Nieminen R.M., Niklasson G.A.,2014, "Nanoparticles of TiO2 and VO2 in dielectric media: Conditions for low optical scattering, and comparison between effective medium and four-flux theories", Solar Energy Materials And Solar Cells, 130, pp. 132-137.
45. Vargas W. E., 1997, "Light Scattering And Absorption In Pigmented Coatings: Theory And Experiments." Ph.D. thesis, Uppsala University, Sweden.

List of Figures

List of Tables